Proceedings of the
44th IEEE Conference on Decision and Control, and
the European Control Conference 2005
Seville, Spain, December 12-15, 2005

Active Suspension Control to Improve Vehicle Ride and Steady-State Handling

Jun Wang, David A. Wilson, Wenli Xu, David A. Crolla

Abstract— **In this paper, a full-vehicle active suspension system is designed to simultaneously improve vehicle ride comfort and steady-state handling performance. First, a linear suspension model of a vehicle and a nonlinear handling model are described. Next, the link between the suspension model and vehicle steady-state handling characteristics is analysed. Then, an H-infinity controller for the suspension is designed to achieve integrated ride-comfort and handling control. Finally, the controller is verified by computer simulations.**

I. Introduction

Although active suspension control has been widely studied for decades, most of the research focussed on vehicle ride comfort, with only a few papers [1–3] and some references cited therein studying how an active suspension can improve vehicle handling.

Ride comfort of a vehicle, also known as vibration isolation ability, is judged by the level of acceleration, which vehicle passengers are exposed to. Since the manner in which vibration affects comfort is dependent on the vibration frequency, frequency weighting functions are used for a fair judgement. Although vehicle ride comfort is somehow a subjective issue, it is quantified by the energy of the weighted vehicle body acceleration [4].

The most common measure of vehicle steady-state handling performance is the understeer gradient [5], by which vehicles are categorised into three types: neutral steer, understeer and oversteer. In the neutral steer case, the lateral acceleration at the gravity centre of the vehicle will yield an identical increase in slip angle at both front and rear wheels. In the understeer case, the lateral acceleration will cause more front-wheel slip. Oversteer is the opposite of understeer. An oversteer vehicle could lose its directional stability at the critical speed. Neutral steer is an ideal steering condition. However, vehicles are generally designed to be understeered for safety since vehicle understeer gradient varies due to transient manoeuvres.

This paper studied the influence of roll moment on vehicle steady-state handling. The roll moment caused by vehicle cornering will transfer vehicle weight from its inside to its outside. Due to the nonlinear nature of tyres, the lateral normal load transfer on the front or rear axle reduces the lateral force generated on its axle. Thus more roll moment distribution on the front axle will cause the vehicle understeer and more on the rear will cause oversteer. Since the rear suspension of a vehicle is generally designed to be stiffer than the front one for reduced pitch vibration [5, 6], roughly speaking the vehicle unfortunately tends to be oversteered. An active suspension provides an opportunity to change roll moment distribution on front and rear axles actively and hence the steady-state handling of the vehicle.

[1] analysed the nonlinear relationship between lateral and normal force of a tyre and designed a nonlinear control law of roll moment distribution. [2] decoupled a full vehicle model into four subsystems, one of which was related to vehicle handling. A nonlinear controller for the suspension was then designed in [3] to improve yaw rate. The problem of handling control by active suspensions was well studied in these papers. However, improvement in suspension ride comfort was not considered and it remains unsure how controllers for ride comfort can work with those *nonlinear* ones for handling. In this paper, a nonlinear tyre model is utilised to transform the nonlinear handling control objective into a linear one, which is later incorporated into the $\mathcal{H}_\infty$ suspension control framework for improved ride and steady-state handling.

The paper is organised as follows. Section II describes models of vehicle suspension and handling systems and Section III derives a linear relationship between the suspension model and the steady-state handling performance. The relationship is then utilised for controller design in Section IV, and the controller performance is evaluated in SectionV by computer simulations. Conclusion is finally made in Section VI.

II. Modelling of Full Vehicle with Active Suspensions

A. Active Suspension Model

A schematic diagram of a full-vehicle model with an active suspension system [7] is shown in Fig. 1.

Each quarter of the active suspension consists of a spring, a damping valve and a force generator connected in parallel. The force generator is regulated by a controller to improve vehicle ride and handling, while the spring and damper are employed to suppress high frequency vibration above the bandwidth of the force generator.

The symbols of the vehicle model is listed in Table I and the differential equations are given as follows [7]:

An extended version of this paper has been submitted to the *International Journal of Vehicle Design.*

J. Wang is with the Department of Automation, Tsinghua University, Beijing, 100084, P R China jwang@ieee.org

D. A. Wilson is with the School of Electronic & Electrical Engineering, The University of Leeds, Leeds LS2 9JT, UK D.A.Wilson@leeds.ac.uk

W. Xu is with the Department of Automation, Tsinghua University, Beijing, 100084, P R China xuwl@mail.tsinghua.edu.cn

D. A. Crolla is with the School of Mechanical Engineering, The University of Leeds, Leeds LS2 9JT, UK D.A.Crolla@leeds.ac.uk

0-7803-9568-9/05/$20.00 ©2005 IEEE

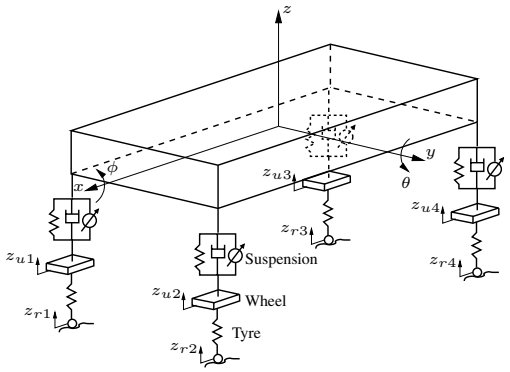

Fig. 1. Schematic diagram of a full-vehicle model

TABLE I
VEHICLE MODEL SYMBOLS

Symbols	Physical meanings
m_s	vehicle sprung mass
m_{ui}	vehicle ith unsprung mass
I_x, I_y, I_z	roll, pitch and yaw moment of inertial
c_{si}	damping ratio of the ith suspension
k_{si}	stiffness of the ith suspension spring
k_u	stiffness of tyre
z_{usi}	the ith suspension deflection
z_{ui}	the ith wheel vertical displacement
z_{ri}	vertical road displacement on the ith wheel
z_{rui}	the ith tyre deflection
F_i	force generated by the ith actuator
l_f, l_r	distance from vehicle GC to front/rear axle
l	distance from vehicle front axle to rear axle
w	half of wheelbase

1) Vehicle body (sprung mass) movements:

$$m_s\ddot{z} = -\sum_{i=1}^{4}\left(k_{si}z + c_{si}\dot{z}\right) + \left(\sum_{i=1}^{2} l_f k_{si} - \sum_{i=3}^{4} l_r k_{si}\right)\theta + \left(\sum_{i=1}^{2} l_f c_{si} - \sum_{i=3}^{4} l_r c_{si}\right)\dot{\theta} + \sum_{i=1}^{4}\left(k_{si}z_{ui} + c_{si}\dot{z}_{ui}\right) + \sum_{i=1}^{4} F_i$$

$$I_y\ddot{\theta} = l_f\sum_{i=1}^{2} k_{si}z - l_r\sum_{i=3}^{4} k_{si}z + l_f\sum_{i=1}^{2} c_{si}\dot{z} - l_r\sum_{i=3}^{4} c_{si}\dot{z} - l_f^2\sum_{i=1}^{2} k_{si}\theta - l_r^2\sum_{i=3}^{4} k_{si}\theta - l_f^2\sum_{i=1}^{2} c_{si}\dot{\theta} - l_r^2\sum_{i=3}^{4} c_{si}\dot{\theta} - l_f\sum_{i=1}^{2}\left(k_{si}z_{ui} + c_{si}\dot{z}_{ui} + F_i\right) + l_r\sum_{i=3}^{4}\left(k_{si}z_{ui} + c_{si}\dot{z}_{ui} + F_i\right)$$

$$I_x\ddot{\phi} = -w^2\sum_{i=1}^{4}\left(k_{si}\phi + c_{si}\dot{\phi}\right) + w\sum_{i=1}^{4}\left((-1)^i\left(k_{si}z_{ui} + c_{si}\dot{z}_{ui} + F_i\right)\right) + M_r$$

2) Wheel (unsprung mass) movements:

$$m_{u1}\ddot{z}_{u1} = k_{s1}z + c_{s1}\dot{z} - l_f k_{s1}\theta - l_f c_{s1}\dot{\theta} - wk_{s1}\phi - wc_{s1}\dot{\phi} - (k_{s1}+k_u)z_{u1} - c_{s1}\dot{z}_{u1} + k_u z_{r1} - F_1$$

$$m_{u2}\ddot{z}_{u2} = k_{s2}z + c_{s2}\dot{z} - l_f k_{s2}\theta - l_f c_{s2}\dot{\theta} + wk_{s2}\phi + wc_{s2}\dot{\phi} - (k_{s2}+k_u)z_{u2} - c_{s2}\dot{z}_{u2} + k_u z_{r2} - F_2$$

$$m_{u3}\ddot{z}_{u3} = k_{s3}z + c_{s3}\dot{z} + l_r k_{s3}\theta + l_r c_{s1}\dot{\theta} - wk_{s3}\phi - wc_{s3}\dot{\phi} - (k_{s3}+k_u)z_{u3} - c_{s3}\dot{z}_{u3} + k_u z_{r3} - F_3$$

$$m_{u4}\ddot{z}_{u4} = k_{s4}z + c_{s4}\dot{z} + l_r k_{s4}\theta + l_r c_{s4}\dot{\theta} + wk_{s4}\phi + wc_{s4}\dot{\phi} - (k_{s4}+k_u)z_{u4} - c_{s4}\dot{z}_{u4} + k_u z_{r4} - F_4$$

By choosing the following vectors of state, disturbance and control signals

$$\mathbf{x} = \begin{bmatrix} z & \dot{z} & \theta & \dot{\theta} & \phi & \dot{\phi} & z_{u1} & \dot{z}_{u1} & z_{u2} & \dot{z}_{u2} & z_{u3} & \dot{z}_{u3} & z_{u4} & \dot{z}_{u4}\end{bmatrix}^T$$
$$\mathbf{w} = \begin{bmatrix} z_{r1} & z_{r2} & z_{r3} & z_{r4} & M_r\end{bmatrix}^T$$
$$\mathbf{u} = \begin{bmatrix} F_1 & F_2 & F_3 & F_4\end{bmatrix}^T$$

we obtain the state equation for the active suspension system

$$\dot{\mathbf{x}} = \mathbf{A}\mathbf{x} + \mathbf{B_w}\mathbf{w} + \mathbf{B_u}\mathbf{u} \tag{1}$$

B. Vehicle Handling Model

The vehicle total mass is $m_t = m_s + \sum_{i=1}^{4} m_{ui}$ and the static normal loads on four wheels are respectively

$$N_{10} = N_{20} = \frac{l_r}{2l}m_t g, \quad N_{30} = N_{40} = \frac{l_f}{2l}m_t g$$

where g is the acceleration of gravity.

Define

$$N_{f0} \triangleq N_{10} + N_{20}, \qquad N_{r0} \triangleq N_{30} + N_{40}$$

The side force developed by the front/rear tyres can be combined to yield the side force of the front/rear axle. Define $F_{yf} \triangleq F_{y1} + F_{y2}$ and $F_{yr} \triangleq F_{y3} + F_{y4}$. By assuming the vehicle longitudinal velocity v_x constant, the handling characteristics of a bicycle-model vehicle in Figure 2 can be described by

$$\begin{cases} m_t\dot{v}_y &= F_{yf} + F_{yr} - m_t v_x^2/r \\ I_z\dot{\omega} &= l_f F_{yf} - l_r F_{yr} \end{cases}$$

where r is a vehicle turning radius. Note that here we follow the tradition [5, 6] and assume small steering and slip angles for a convenient analysis.

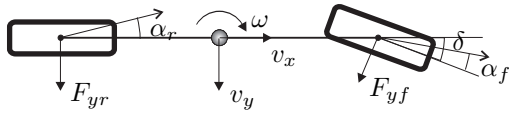

Fig. 2. Simplified steady-state handling model

When the vehicle reaches its steady state, i.e. $\dot{v}_y = 0$ and $\dot{\omega} = 0$, we have

$$\begin{cases} F_{yf} + F_{yr} - m_t v_x^2/r &= 0 \\ F_{yf} l_f - F_{yr} l_r &= 0 \end{cases}$$

i.e.

$$F_{yf} = \frac{l_r m_t v_x^2}{l\, r}, \qquad F_{yr} = \frac{l_f m_t v_x^2}{l\, r} \tag{2}$$

In this paper, we follow [1, 5] and use a second-order polynomial, also known as an empirical formula, to describe the nonlinear relationship between tyre lateral force and normal load. The lateral force generated on the front and rear axles are respectively

$$\begin{aligned} F_{yf} &= \left[C_1(N_{10}+N_{20}) + C_2(N_{10}^2+N_{20}^2)\right]\alpha_f \\ &= \left(C_1 N_{f0} + \frac{1}{2}C_2 N_{f0}^2\right)\alpha_f \end{aligned} \tag{3}$$

$$\begin{aligned} F_{yr} &= \left[C_1(N_{30}+N_{40}) + C_2(N_{30}^2+N_{40}^2)\right]\alpha_r \\ &= \left(C_1 N_{r0} + \frac{1}{2}C_2 N_{r0}^2\right)\alpha_r \end{aligned} \tag{4}$$

where α_f and α_r are respectively front- and rear-wheel slip angles, and C_1 and C_2 satisfying $C_1 \gg -C_2 > 0$ are empirical coefficients decided from tyre experimental data.

Define

$$C_{f0} \triangleq C_1 N_{f0} + \frac{1}{2}C_2 N_{f0}^2$$

$$C_{r0} \triangleq C_1 N_{r0} + \frac{1}{2}C_2 N_{r0}^2$$

Note that C_{f0} and C_{r0} are the well-known cornering stiffness of the front and the rear tyres when there is no lateral load transfer in the vehicle. The equations (8) and (9) can be rewritten as $F_{yf} = C_{f0}\alpha_f$ and $F_{yr} = C_{r0}\alpha_r$.

From (2), (3) and (4), we have

$$\alpha_f - \alpha_r = \left(\frac{l_r}{C_{f0}} - \frac{l_f}{C_{r0}}\right)\frac{m_t g}{l} \cdot \frac{v_x^2}{gr} \tag{5}$$

By the definition given in [5, p.202] and [6, p.287], the understeer gradient of the vehicle is

$$K_{us0} = \left(\frac{l_r}{C_{f0}} - \frac{l_f}{C_{r0}}\right)\frac{m_t g}{l} \tag{6}$$

when there is no lateral normal-load transfer. For clarity, K_{us0} is also called in this paper the *static* understeer gradient.

III. Link between Active Suspension and Handling

When the vehicle is turning with a radius r at a constant speed v_x, the roll moment due to the inertial centrifugal force is $M_r = \frac{m_t v_x^2 h_r}{r}$, where h_r is the height of the vehicle roll centre. The roll moment causes the vehicle load transfer from its inside to its outside, and the lateral load transfer produces roll moment to react against M_r.

Suppose the roll moment distributed on the front and the rear axles is εM_r and $(1-\varepsilon)M_r$ respectively, where $\varepsilon \in (0, 1)$. The load transfers on the front and the rear axles then become

$$N_{\Delta f} = \frac{\varepsilon M_r}{w} = \frac{\varepsilon m_s v_x^2 h_r}{w\, r}$$

$$N_{\Delta r} = \frac{(1-\varepsilon)M_r}{w} = \frac{(1-\varepsilon) m_s v_x^2 h_r}{w\, r}$$

and

$$\frac{N_{\Delta f}}{N_{\Delta r}} = \frac{\varepsilon}{(1-\varepsilon)} \tag{7}$$

Then the normal loads on the wheels are

$$N_1 = N_{10} + \frac{1}{2}N_{\Delta f}, \qquad N_2 = N_{20} - \frac{1}{2}N_{\Delta f}$$

$$N_3 = N_{30} + \frac{1}{2}N_{\Delta r}, \qquad N_4 = N_{40} - \frac{1}{2}N_{\Delta r}$$

The lateral force generated on the front and the rear axles is respectively

$$F_{yf} = \left(C_{f0} + \frac{1}{2}C_2 N_{\Delta f}^2\right)\alpha_f \tag{8}$$

$$F_{yr} = \left(C_{r0} + \frac{1}{2}C_2 N_{\Delta r}^2\right)\alpha_r \tag{9}$$

From (2), (8) and (9), we have

$$\alpha_f - \alpha_r = K_{us} \cdot \frac{v_x^2}{g\, r} \tag{10}$$

where the understeer gradient of the vehicle is defined as

$$K_{us} = \left(\frac{l_r}{C_{f0} + \frac{1}{2}C_2 N_{\Delta f}^2} - \frac{l_f}{C_{r0} + \frac{1}{2}C_2 N_{\Delta r}^2}\right)\frac{m_t g}{l} \tag{11}$$

Since $C_1 \gg -C_2 > 0$ and $N_{f0} > N_{\Delta f} > 0$, we have [5]

$$\frac{1}{C_{f0} + \frac{1}{2}C_2 N_{\Delta f}^2} \approx \frac{1}{C_{f0}}\left(1 - \frac{C_2 N_{\Delta f}^2}{2C_{f0}}\right)$$

Similarly we have

$$\frac{1}{C_{r0} + \frac{1}{2}C_2 N_{\Delta r}^2} \approx \frac{1}{C_{r0}}\left(1 - \frac{C_2 N_{\Delta r}^2}{2C_{r0}}\right)$$

Then

$$K_{us} \approx K_{us0} - \left(\frac{l_r C_2 N_{\Delta f}^2}{2C_{f0}^2} - \frac{l_f C_2 N_{\Delta r}^2}{2C_{r0}^2}\right)\frac{m_t g}{l} \tag{12}$$

From (12), we obtain that $K_{us} \approx K_{us0}$ if

$$\frac{N_{\Delta f}}{N_{\Delta r}} = \frac{\sqrt{l_f} C_{f0}}{\sqrt{l_r} C_{r0}} \tag{13}$$

Now we conclude from (7) and (13) that $K_{us} \approx K_{us0}$ if

$$\frac{\varepsilon}{1-\varepsilon} = \frac{\sqrt{l_f} C_{f0}}{\sqrt{l_r} C_{r0}} \tag{14}$$

In this paper, the tyre is modelled as a spring and the roll moment generated by the front and the rear pairs of tyres is respectively

$$\begin{aligned} k_u(z_{ru1} - z_{ru2})w &= -\varepsilon M_r \\ k_u(z_{ru3} - z_{ru4})w &= -(1-\varepsilon)M_r \end{aligned}$$

Hence we have

$$\frac{z_{ru1} - z_{ru2}}{z_{ru3} - z_{ru4}} = \frac{\varepsilon}{1-\varepsilon} \tag{15}$$

From (14) and (15), we obtain the following equation

$$\sqrt{l_r} C_{r0}(z_{ru1} - z_{ru2}) = \sqrt{l_f} C_{f0}(z_{ru3} - z_{ru4}) \tag{16}$$

which lays the foundation for integrated active suspension control.

IV. Integrated Controller Design

In this section, an $\mathcal{H}_\infty$ controller for the active suspension is designed to achieve improved ride comfort and handling performance simultaneously.

A. Multiple Control Goals

An active suspension system is designed to effectively isolate the vibration caused by road irregularities while constraining the suspension to move within a limited space and guaranteeing good road-tyre contact. It can also improve handling performance, as shown in [1, 3]. As the understeer gradient is the most important measure of the steady-state handling performance, the active suspension is employed here to keep the vehicle working in slightly understeer and nearly neutral steer condition when the vehicle is steered at high speed. Thus the control objectives of this design are ride and handling performance, and suspension travel and road holding ability are evaluated after the design.

B. Output Selection

The ride comfort is quantified by the energy of weighted vehicle body acceleration $\ddot{z}$, $\ddot{\theta}$ and $\ddot{\phi}$. From (16), we know that $K_{us} \approx K_{us0}$ if

$$k_f(z_{ru1} - z_{ru2}) - k_r(z_{ru3} - z_{ru4}) = 0$$

where $k_f = \frac{\sqrt{l_r}C_{r0}}{\sqrt{l_r}C_{r0}+\sqrt{l_f}C_{f0}}$ and $k_r = \frac{\sqrt{l_f}C_{f0}}{\sqrt{l_r}C_{r0}+\sqrt{l_f}C_{f0}}$. Hence we also need to minimise handling performance index

$$k_{hpi} \triangleq k_f(z_{ru1} - z_{ru2}) - k_r(z_{ru3} - z_{ru4})$$

so that the understeer characteristics of the vehicle are little affected by steering manoeuvres and external disturbances. In addition, we need to constrain force generated by actuators. Hence we choose the vector of regulated output variables as $\mathbf{z} = \begin{bmatrix}\ddot{z} & \ddot{\theta} & \ddot{\phi} & k_{hpi} & F_1 & F_2 & F_3 & F_4\end{bmatrix}^T$.

The most common sensors for active suspension control are accelerometers, gyrometers and suspension defection sensors [8]. In this paper, we only choose the accelerometers and gyrometers for a simple implementation. To effectively keep the understeer gradient constant, we also need to measure the deflection of tyres, which used to be extremely difficult. Fortunately, recent technology developments [9] have made it possible to measure tyre pressure in production vehicles. As a matter of fact, direct tyre-pressure measurements have been mandated in the North America for driving safety. In this paper, the handling-performance index k_{hpi} needs to be computed from tyre deflection. In summary, we choose the vector of measuring signals as $\mathbf{y} = \begin{bmatrix}\ddot{z} & \dot{\theta} & \dot{\phi} & k_{hpi}\end{bmatrix}^T$.

Combined with the state equation given in (1), a state-space model $\mathbf{G}$ for the integrated active suspension control is formulated as follows:

$$\begin{cases} \dot{\mathbf{x}} &= \mathbf{A}\mathbf{x} + \mathbf{B_w}\mathbf{w} + \mathbf{B_u}\mathbf{u} \\ \mathbf{z} &= \mathbf{C_z}\mathbf{x} + \mathbf{D_{zw}}\mathbf{w} + \mathbf{D_{zu}}\mathbf{u} \\ \mathbf{y} &= \mathbf{C_y}\mathbf{x} + \mathbf{D_{yw}}\mathbf{w} + \mathbf{D_{yu}}\mathbf{u} \end{cases} \tag{17}$$

where the matrices $\mathbf{C_z}$, $\mathbf{C_y}$, $\mathbf{D_{zw}}$, $\mathbf{D_{zu}}$, $\mathbf{D_{yw}}$ and $\mathbf{D_{yu}}$ are obtained in a straightforward manner.

C. Scaling and Weight Selection

Before designing an $\mathcal{H}_\infty$ controller for the active suspension, we scale the state-space model given in (17) and tune weighting functions for the regulated outputs.

Scaling is important in practical applications as it makes model analysis and controller design much simpler. Scalings are chosen to reflect the allowable magnitude of each disturbance signal and the allowable deviation of each regulated output. In this paper, scaling matrices for $\mathbf{w}$ and $\mathbf{z}$ are respectively tuned as follows:

$$\mathbf{S_w} = \text{diag}(0.0014, 0.0014, 0.0014, 0.0014, 500)$$
$$\mathbf{S_z} = \text{diag}(1, 3, 1, 200, 0.0015, 0.0015, 0.0015, 0.0015)$$

Based on the ISO 2631-1 [4], human sensitivity to vibration dependent on frequency. Humans are more sensitive to vertical acceleration at 4$\sim$ 8 Hz and rotational one at 1$\sim$2 Hz. In $\mathcal{H}_\infty$ control, this frequency-dependent design specification can be easily satisfied by choosing weighting functions for $\ddot{z}$, $\ddot{\theta}$ and $\ddot{\phi}$ as follows:

$$W_{\ddot{z}} = \frac{s^2 + 314.2s + 987}{s^2 + 43.98s + 987}$$
$$W_{\ddot{\theta}} = \frac{s^2 + 50.27s + 25.27}{s^2 + 7.037s + 25.27}, \quad W_{\ddot{\phi}} = W_{\ddot{\theta}}$$

As it is our main concern to minimise the steady-state value of k_{hpi},

$$W_{k_{hpi}} = \frac{s + 50}{s + 1}$$

is chosen as its weighting function. Since we do not have any particular frequency requirements on actuator force, we simply choose $W_u = 1$ as its weighting function. In summary, the weighting function matrix for the regulated output $\mathbf{z}$ is

$$\mathbf{W_z} = \text{diag}(W_{\ddot{z}}, W_{\ddot{\theta}}, W_{\ddot{\phi}}, W_{k_{hpi}}, W_u, W_u, W_u, W_u)$$

D. $\mathcal{H}_\infty$ Control Design

$\mathcal{H}_\infty$ control aims to design a controller $\mathbf{K_{ias}}$ so that the closed-loop system $\mathbf{G_{cl}}$ achieves the minimal $\mathcal{H}_\infty$ norm. The closed-loop system is computed by linear operators, i.e. $\mathbf{G_{cl}} = \mathbf{W_z} \cdot \mathbf{S_z} \cdot \mathcal{F}_l(\mathbf{G_{gel}}, \mathbf{K_{ias}}) \cdot \mathbf{S_w}$, where $\mathcal{F}_l$ stands for a lower linear fractional transformation. The active suspension control problem can be formulated as the following standard one: to compute a controller $\mathbf{K_{ias}}$ so that

$$\min_{\mathbf{K_{ias}}} \sup_{\omega} \Big(\bar{\sigma}\big(\mathbf{G_{cl}}(j\omega)\big) \Big)$$

where $\bar{\sigma}(\cdot)$ stands for the maximal singular value. Such a problem can be solved by a linear-matrix-inequality method given in [10] or the programme 'hinflmi.m' provided by LMI Control Toolbox for Use with MATLAB.

For performance comparison, an ordinary $\mathcal{H}_\infty$ control $\mathbf{K_{as}}$ is also designed for the active suspension. $\mathbf{K_{as}}$ is computed in the same procedures as for $\mathbf{K_{ias}}$ except that the handling performance index is not considered as a control objective.

V. Simulation Results and Analyses

Computer simulations are carried out in this section to evaluate the ride and steady-state handling performance of the vehicle. The active suspension with the integrated H_∞ controller $\mathbf{K_{ias}}$ (denoted by IAS) is compared to the passive suspension (denoted by PS) and the active suspension with the ordinary H_∞ controller $\mathbf{K_{as}}$ (denoted by AS). Simulation parameters are listed in Table II.

TABLE II

Simulation Parameters

Symbol	Value	Unit	Symbol	Value	Unit
m_s	1500	kg	$k_{s1},\ k_{s2}$	35000	N/m
m_{ui}	59	kg	$k_{s3},\ k_{s4}$	38000	N/m
I_x	460	kg m^2	$c_{s1},\ c_{s2}$	1000	Ns/m
I_y	2160	kg m^2	$c_{s3},\ c_{s4}$	1100	Ns/m
I_z	2500	kg m^2	k_u	190000	N/m
l_f	1.4	m	δ	5	degree
l_r	1.7	m	C_1	13.098	1/rad
h_r	0.45	m	C_2	-0.001045	1/(rad N)

Fig. 3 shows the frequency responses of the vehicle vertical, pitch angular and roll angular acceleration to the front-left road disturbance. It is clearly observed that the acceleration of active suspension systems IAS and AS is considerably lower than that of the passive one PS in the frequency range where humans are more sensitive to vibration, so both active systems effectively improve the vehicle ride comfort.

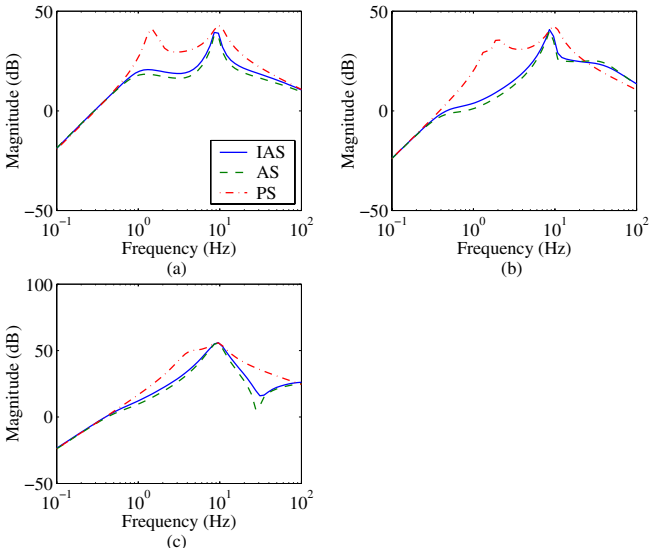

Fig. 3. Magnitude of the frequency response of vehicle acceleration to front-right road displacement z_{r1}: (a) $\ddot{z}$; (b) $\ddot{\theta}$; (c) $\ddot{\phi}$

Fig. 4 shows the frequency response of the vehicle handling performance index K_{hpi} to the roll moment disturbance M_r. Here the roll moment is regarded as an *external* disturbance caused by steering manoeuvres. Since the disturbance M_r is normally of low frequency and, more importantly, the index K_{hpi} is a steady-state index for vehicle cornering performance, the low-frequency response of K_{hpi} to M_r is of more importance. It is observed from Fig. 4 that K_{hpi} of IAS is much less than that of AS and PS in a wide low-frequency range. Hence the IAS system is expected to achieve better steady-state handling performance than the AS and PS systems. This conclusion can be more directly reached in Fig. 5, which shows the time response of K_{hpi} to a unit step signal M_r. The IAS system has lower steady-state value, less overshoot and shorter settling time, while the AS and PS systems have similar steady-state handling performance.

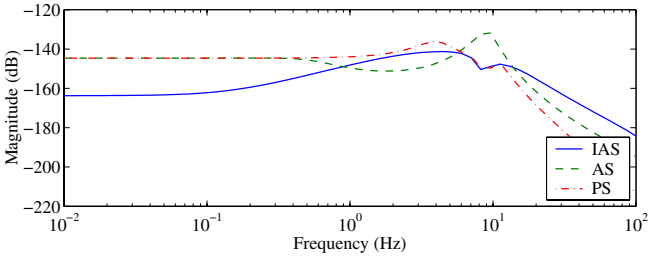

Fig. 4. Magnitude of the frequency response of handling performance index K_{hpi} to external roll moment disturbance M_r

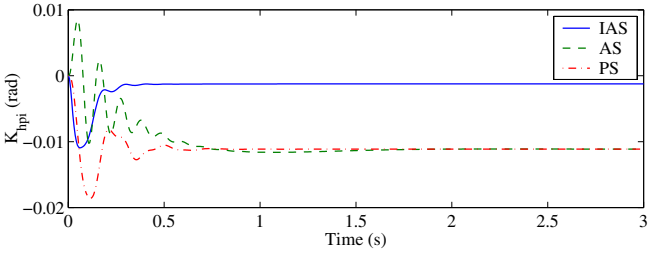

Fig. 5. Step response of handling performance index K_{hpi} to roll moment disturbance M_r

The suspension of a real vehicle can only move within a limited space known as the "rattle space". Road holding ability represented by tyre deflection is important for vehicle handling stability [6]. Large suspension deflection and tyre deflection tend to appear when a vehicle is disturbed by large roll and/or pitch moment. Since suspension deflection and tyre deflection are an important aspect of suspension performance and are not addressed in the controller design, we now study the frequency responses of the suspension and tyre deflection to the roll moment disturbance.

As shown in Fig. 6, the IAS and the AS systems have responses of suspension deflection similar to those of the PS system in the frequency ranges below the natural frequency of sprung mass and above that of unsprung mass. However, in the mid-frequency range, the suspension deflection of IAS and AS is considerably reduced. Therefore, the active systems IAS and AS require less rattle space than the passive one.

Fig. 7 shows that the IAS, the AS and the PS systems have similar frequency responses of tyre deflection in the frequency range below the natural frequency of unsprung mass. In the frequency range above, the magnitude of all the systems' responses dramatically decays with the increase

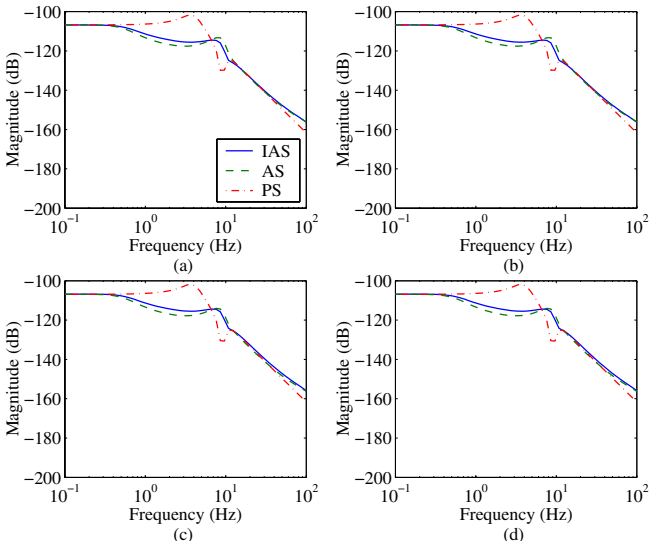

Fig. 6. Magnitude of the frequency response of vehicle suspension deflection to external roll moment disturbance M_r: (a) z_{us1}; (b) z_{us2}; (c) z_{us3}; (d) z_{us4}b

of the frequency. Although the decay rate of PS is larger than those of IAS and AS, it has little effect on vehicle tyre deflection dynamics. Hence the IAS, the AS and the PS systems have similar road holding ability.

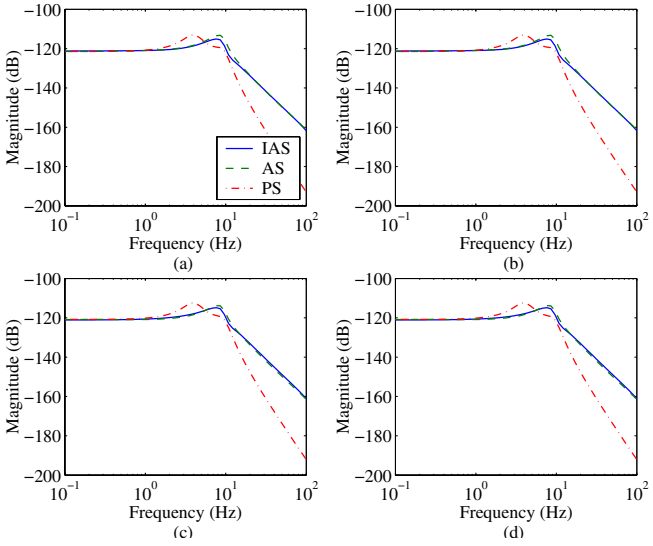

Fig. 7. Magnitude of the frequency response of vehicle tyre deflection to external roll moment disturbance M_r: (a) z_{ru1}; (b) z_{ru2}; (c) z_{ru3}; (d) z_{ru4}

It is also observed that the force generated by the actuators to achieve the above performance is within ± 1000 N, which is below the standard limit ± 8000 N [3].

In summary, the integrated $\mathcal{H}_\infty$ controller simultaneously improves vehicle ride comfort and handling performance with low actuator energy consumption.

VI. Conclusions

This paper designs an $\mathcal{H}_\infty$ controller for the active suspension system to simultaneously improve vehicle ride comfort and steady-state handling performance.

The nonlinear effect of roll moment distribution on vehicle handling is transformed into a linear control objective, which can be easily incorporated into general suspension control frameworks and achieved by linear control strategies.

The integrated controller can preserve vehicle handling characteristics, regardless of lateral acceleration changes due to driving manoeuvres such as forward speed changes. Vehicles in the market are generally designed to be understeer and sometimes are equipped with anti-roll bars for a sufficient safety margin although neutral steer is in accord with human intuition of cornering. The research presented in this paper provides the opportunity to design a slightly understeered and nearly neutral-steered vehicle. The control strategy can improve handling without sacrificing vehicle cornering stability, and it can in fact reinforce vehicle steering safety as shown in the simulations.

In the future, a more generalised case will be considered. For example, it will be unnecessary for tyres to be identical and actuator dynamics will be incorporated into the design.

Acknowledgements

This research was sponsored in part by Scientific Research Foundation for Returned Overseas Scholars by State Education Ministry, Postdoctoral Science Foundation of China under Grant No. 2004035058, Natural Science Foundation of China under Grant No. 50275045 and No. 50411130486, and Royal Society of UK under Grant No. 16558.

The authors are grateful to anonymous reviewers for their insightful comments and valuable suggestions.

References

[1] D. E. Williams and W. M. Haddad, "Nonlinear control of roll moment distribution to influence vehicle yam characteristics," *IEEE Transactions on Control Systems Technology*, vol. 3, no. 1, pp. 110–116, March 1995.

[2] M. Lakehal-Ayat, S. Diop, and E. Fenaux, "Development of a full active suspension system," in *Proceedings of 15th Triennial World Congress of the International Federation of Automatic Control*. Barcelona: IFAC, July 2002, paper No. 2658.

[3] ——, "An improved active suspension yaw rate control," in *Proceedings of the American Control Conference*, 2002, pp. 863–868.

[4] ISO 2631-1, *Mechanical vibration and shock — Evaluation of human exposure to whole-body vibration — Part 1: General requirements*, 2nd ed., International Standards Organization, 1997.

[5] T. D. Gillispie, *Fundamentals of Vehicle Dynamics*. Warrendale, PA, USA: Society of Automotive Engineers, Inc., 1992.

[6] J. Y. Wong, *Theory of Ground Vehicles*, 2nd ed. John Wiley & Sons, Inc., 1993.

[7] S. Ikenaga, F. L. Lewis, J. Campos, and L. Davis, "Active suspension control of ground vehicle based on a full-vehicle model," in *Proceedings of the American Control Conference*, 2000, pp. 4019–4024.

[8] C. O. Nwagboso, Ed., *Automotive sensory systems*, ser. Road Vehicle Automation. Chapman & Hall, 1993.

[9] The APOLLO Consortium, "Intelligent tyre for accident-free traffic," Technical Research Centre of Finland (VTT), Tech. Rep., May 2003, project No: IST-2001-34372.

[10] J. Wang, D. A. Wilson, and G. D. Halikias, "H_∞ robust-performance control of decoupled active suspension systems based on LMI method," in *Proceedings of the American Control Conference*, 2001, pp. 2658–2663.